

Supplementary Material

S.1 Hyperparameter Selection: PISCO Weighting Factor λ

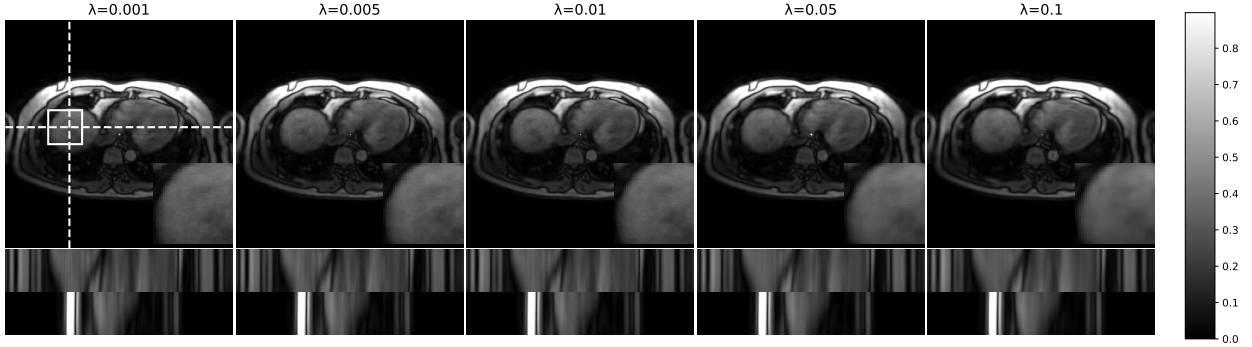


Figure S.1: Influence of PISCO weighting factor λ on an exemplary slice of the **abdominal** dataset. Increasing smoothing is visible with increasing λ (left to right). Therefore, $\lambda = 0.01$ is selected for this dataset as a tradeoff between little effect of the regularization (left) and oversmoothing (right). The same procedure is applied for the remaining datasets.

S.2 Training Details

Model	DIP-based		INR-based			
	TD-DIP128	TD-DIP512	NIK	ICoNIK	PISCO-dist	PISCO-res
Parameters [Million]	1.333	1.924	1.067	1.074	1.067	1.067
Total Size [MB]	94.99	1443.49	4.29	4.29	4.29	4.29
Training Time [min]	6.85	10.97	17.05	19.42	42.83	22.30

Table S.1: Training details for all learning-based dynamic reconstruction models computed on one cardiac cine subject. DIP-based methods enable fast training but are restricted to a fixed spatial output resolution. As the target resolution increases (TD-DIP512), these models require more parameters and memory. In contrast, INR-based approaches can reconstruct images at arbitrary resolutions once trained, offering greater flexibility while maintaining a compact model size—requiring only a fraction of the memory used by DIP-based methods. Although NIK currently requires longer training than TD-DIP512, further GPU optimization for MLP training (as opposed to CNNs) is expected to reduce this gap. ICoNIK, a lightweight post-processing extension to NIK, adds only 10% additional training time by fitting a kernel to NIK’s output. However, its performance may be limited at high acceleration rates due to inaccuracies in kernel estimation. Compared to PISCO-dist, the proposed PISCO-res regularization improves reconstruction quality while increasing training time by only 30%, rather than doubling it. Additional gains are anticipated with further optimization of the weight solving.

S.3 Quantitative Results - Cardiac Cine

Acc. Factor	NUFFT25	XD-GRASP25	TD-DIP128	TD-DIP512	NIK	ICoNIK	PISCO-dist	PISCO-res
R15	18.94 \pm 1.65	29.96 \pm 2.10	24.45 \pm 1.60	<i>28.87</i> \pm <i>2.06</i>	26.90 \pm 2.02	23.09 \pm 2.02	26.89 \pm 2.01	27.00 \pm 1.97
R26	16.20 \pm 1.23	<i>27.96</i> \pm <i>1.95</i>	24.16 \pm 1.63	28.08 \pm 2.02	26.55 \pm 2.12	22.83 \pm 2.10	26.60 \pm 2.04	26.83 \pm 1.85
R52	14.14 \pm 0.87	<i>25.37</i> \pm <i>1.64</i>	23.44 \pm 1.77	26.84 \pm 2.01	23.08 \pm 2.72	20.34 \pm 2.65	23.75 \pm 2.65	25.31 \pm 1.96
R104	13.10 \pm 0.72	21.59 \pm 1.45	22.33 \pm 1.94	25.11 \pm 1.97	16.78 \pm 2.46	15.22 \pm 2.31	18.50 \pm 2.69	<i>22.36</i> \pm <i>1.77</i>

Table S.2: PSNR results

Acc. Factor	NUFFT25	XD-GRASP25	TD-DIP128	TD-DIP512	NIK	ICoNIK	PISCO-dist	PISCO-res
R15	0.58 \pm 0.03	0.80 \pm 0.02	0.70 \pm 0.02	<i>0.76</i> \pm <i>0.03</i>	0.75 \pm 0.02	0.71 \pm 0.03	0.75 \pm 0.02	0.75 \pm 0.02
R26	0.50 \pm 0.02	0.77 \pm 0.02	0.69 \pm 0.02	0.75 \pm 0.03	0.74 \pm 0.02	0.70 \pm 0.04	0.75 \pm 0.02	<i>0.75</i> \pm <i>0.02</i>
R52	0.44 \pm 0.02	<i>0.72</i> \pm <i>0.02</i>	0.67 \pm 0.02	0.73 \pm 0.03	0.68 \pm 0.04	0.63 \pm 0.05	0.69 \pm 0.04	0.72 \pm 0.03
R104	0.42 \pm 0.01	0.65 \pm 0.02	0.65 \pm 0.03	0.70 \pm 0.03	0.52 \pm 0.06	0.48 \pm 0.06	0.57 \pm 0.06	<i>0.66</i> \pm <i>0.02</i>

Table S.3: FSIM spatial results

Acc. Factor	NUFFT25	XD-GRASP25	TD-DIP128	TD-DIP512	NIK	ICoNIK	PISCO-dist	PISCO-res
R15	0.49 \pm 0.03	0.67 \pm 0.03	0.61 \pm 0.02	<i>0.67</i> \pm <i>0.03</i>	0.64 \pm 0.03	0.61 \pm 0.03	0.64 \pm 0.03	0.64 \pm 0.03
R26	0.42 \pm 0.03	0.62 \pm 0.02	0.59 \pm 0.02	0.64 \pm 0.03	0.61 \pm 0.03	0.58 \pm 0.04	0.61 \pm 0.03	<i>0.62</i> \pm <i>0.03</i>
R52	0.37 \pm 0.02	0.57 \pm 0.02	0.55 \pm 0.03	0.60 \pm 0.03	0.52 \pm 0.04	0.49 \pm 0.05	0.54 \pm 0.04	<i>0.58</i> \pm <i>0.03</i>
R104	0.34 \pm 0.02	0.51 \pm 0.02	0.51 \pm 0.03	0.56 \pm 0.03	0.40 \pm 0.04	0.38 \pm 0.04	0.43 \pm 0.04	<i>0.52</i> \pm <i>0.03</i>

Table S.4: FSIM temporal results